ACTA OCEANOGRAPHICA TAIWANICA VOL.37, NO.2, PP.139-164, 2 TABS. 12 FIGS., SEPTEMBER 1998

The role of the Taiwan Strait in an Ecological Model in the East China Sea

Xinyu Guo [1] and Tetsuo Yanagi [2]

(received 1998/2/17, revised 1998/5/8, accepted 1998/5/18)

ABSTRACT

An ecological model, which has reproduced the major distribution characteristics of the observed DIN (Dissolved Inorganic Nitrogen), DIP (Dissolved Inorganic Phosphate), phytoplankton, zooplankton and detritus in April 1994 in the East China Sea (ECS), is used to examine the role of the Taiwan Strait in the ecosystem of the ECS, especially focusing on its volume transport. The nutrients (DIN and DIP) in the ECS are assumed to have three sources, that are the rivers (mainly Changjiang), the Taiwan Strait and the shelf edge. To estimate the contributions of the above three sources of DIN and DIP in the ECS, they are labeled in the ecological model. The separation of the nonlinear biochemical terms in the ecological model is based on the content ratio of the three sources of DIN and DIP in a grid. The numerical model shows that the variation of the volume transport through the Taiwan Strait influences the nutrient supplies in the ECS largely, but has little influence on the primary production there. This is because the change in the import of nutrients from the Taiwan Strait may be compensated by the nutrients input from the shelf edge.

(Keywords: Taiwan Strait, ecological model, East China Sea)

INTRODUCTION

Modeling techniques of an ecosystem in the ocean or a coastal water have been developed for many years (Steele, 1974). At present, many ecological models have been established (Kremer and Nixon, 1978; Baretta and Ruardij, 1989; Fasham et al., 1990) and applied to the prediction of water

[1] Institute for Global Change Research, SEAVANS North 7F, 2-8-1 Shibaura, Minato-ku, Tokyo 105-6791, Japan

[2] Research Institute for Applied Mechanics, Kyushu University,6-1 Kasuga-kohen, Kasuga-city, Fukuoka 816-8580, Japan

quality in a bay (Nakata, 1993), 'Red Tide' problem (Kishi and Ikeda, 1986) and management of a heavy polluted bay (Yanagi et al., 1997). It may be said that the ecological model has been capable of simulating the natural ecological system with fair precision.

In Guo et al. (1997), an ecological model including DIN (Dissolved Inorganic Nitrogen), DIP (Dissolved Inorganic Phosphate), phytoplankton, zooplankton and detritus, is developed and applied to the East China Sea (ECS). Using this ecological model, the major characteristics of the observed DIN, DIP, Chl.a and detritus in April 1994 in the ECS were reproduced and some important results were obtained.

However, due to the limited amount of data, there are some unclear points in this model. One of them is the volume transport through the Taiwan Strait. At present, there are two viewpoints about the volume transport through the Taiwan Strait. One is that about 1 Sv (= 1 x $10^6 m^3/s$) water in winter and 3 Sv water in summer pass through the Taiwan Strait northward, respectively (Fang et al., 1991; Fu et al., 1991). Its annual mean is therefore 2 Sv. It should be noted that Fang et al. (1991) and Fu et al. (1991) used different observed current data but obtained a similar conclusion. On the other hand, this viewpoint may be supported indirectly by the observation and the numerical experiments on the Tsushima/Korea current (Isobe, 1994, 1997). Therefore this value was used in our ecological model in the ECS (Guo et al., 1997).

A viewpoint in Chemical oceanography says that it is impossible to have averaged more than 1 Sv of water passing through the Taiwan Strait annually (Chen, personal communication). In Chen and Wang (1997), a small volume transport (0.5Sv for May to October and 0.2Sv for November to April) is used to calculate the nutrients budget in the ECS.

So, though we believed that the viewpoint of 2 Sv is a relatively robust conclusion, we still want to examine the influence of the change of the volume transport through the Taiwan strait on our ecological model, because the observed current data and observation period in Fang et al. (1991) or Fu et al. (1991) are also limited.

In this paper, the residual current is first calculated by a robust diagnostic model, using the different volume transport through the Taiwan Strait, respectively. Then, the ecological model is run in the two residual flow fields, respectively, and two quasi-steady solutions of the five compartments are obtained. By comparing these two solutions, the role of the Taiwan Strait is discussed.

PHYSICAL PROCESSES

Before we run the ecological model, we must first build a physical field including the residual

current and the tidal current. The tidal current has little relation to the density field and the wind and was calculated in advance (Guo and Yanagi, 1997). As for the residual current, it may be calculated by a robust diagnostic model (Yanagi and Takahashi, 1993; Guo and Yanagi, 1996) using the observed water temperature, salinity and wind data in April, 1994. Figure 1 shows the horizontal distribution of the observed temperature, salinity and density (σ_t) at the depth of 10 m. It must be noted that the data north to Cheju Inland are drawn from Yanagi and Takahashi (1993) which are the climatological state in Spring.

MODEL AND THE BOUNDARY CONDITIONS

The basic equations in the Cartesian coordinate system, with x axis eastward, y axis northward and z axis upward from the mean sea surface, are:

$$\frac{\partial u}{\partial t}+\vec{u}\cdot\nabla u-fv=-\frac{1}{\rho_0}\frac{\partial P}{\partial x}+\frac{\partial}{\partial z}\left(A_v\frac{\partial u}{\partial z}\right)+\frac{\partial}{\partial x}\left(A_h\frac{\partial u}{\partial x}\right)+\frac{\partial}{\partial y}\left(A_h\frac{\partial u}{\partial y}\right) \tag{1}$$

$$\frac{\partial v}{\partial t}+\vec{u}\cdot\nabla v+fu=-\frac{1}{\rho_0}\frac{\partial P}{\partial y}+\frac{\partial}{\partial z}\left(A_v\frac{\partial v}{\partial z}\right)+\frac{\partial}{\partial x}\left(A_h\frac{\partial v}{\partial x}\right)+\frac{\partial}{\partial y}\left(A_h\frac{\partial v}{\partial y}\right) \tag{2}$$

$$P=\rho_0 g(\eta-z)+\rho_0 g\int_z^0\frac{\rho-\rho_0}{\rho_0}dz' \tag{3}$$

$$\frac{\partial \eta}{\partial t}+\frac{\partial}{\partial x}\int_{-h}^{0}udz+\frac{\partial}{\partial y}\int_{-h}^{0}vdz=0 \tag{4}$$

$$\rho=F(T,S) \tag{5}$$

$$\frac{\partial T}{\partial t}+\vec{u}\cdot\nabla T=\frac{\partial}{\partial x}\left(K_h\frac{\partial T}{\partial x}\right)+\frac{\partial}{\partial y}\left(K_h\frac{\partial T}{\partial y}\right)+\frac{\partial}{\partial z}\left(K_v\frac{\partial T}{\partial z}\right)+\gamma(T^*-T) \tag{6}$$

$$\frac{\partial S}{\partial t}+\vec{u}\cdot\nabla S=\frac{\partial}{\partial x}\left(K_h\frac{\partial S}{\partial x}\right)+\frac{\partial}{\partial y}\left(K_h\frac{\partial S}{\partial y}\right)+\frac{\partial}{\partial z}\left(K_v\frac{\partial S}{\partial z}\right)+\gamma(S^*-S) \tag{7}$$

where

$$\vec{u}=u\vec{i}+v\vec{j}+w\vec{k}$$

$$\nabla=\vec{i}\frac{\partial}{\partial x}+\vec{j}\frac{\partial}{\partial y}+\vec{k}\frac{\partial}{\partial z}$$

u and v are the eastward and northward velocity; η the sea surface elevation from the mean sea surface; T and S the water temperature and salinity; T* and S* the observed water temperature and salinity; ρ the density and ρ_0 the reference density; $f = f_0 + \beta y$ ($f_0 = 7.73 \times 10^{-5}$ s^{-1} at 32°N, $\beta = 1.94 \times 10^{-13}$ s^{-1} cm^{-1}) the Coriolis parameter; g (= 980 cms^{-2}) gravitational acceleration; A_h, A_v, the horizontal and vertical eddy viscosity; K_h, K_v the horizontal and vertical eddy diffusivity; h is the water depth. (5) is the well known Knudsen state equation. The last terms in (6) and (7) are called γ terms, which are introduced by Sarmiento and Bryan (1982) to prevent calculated values T and S from deviating greatly from observed values T* and S* Also it can remove the noise in the interpolated water temperature and salinity data and make the calculated water temperature and salinity smooth (Sarmiento and Bryan, 1982; Fujio and Imasato, 1991).

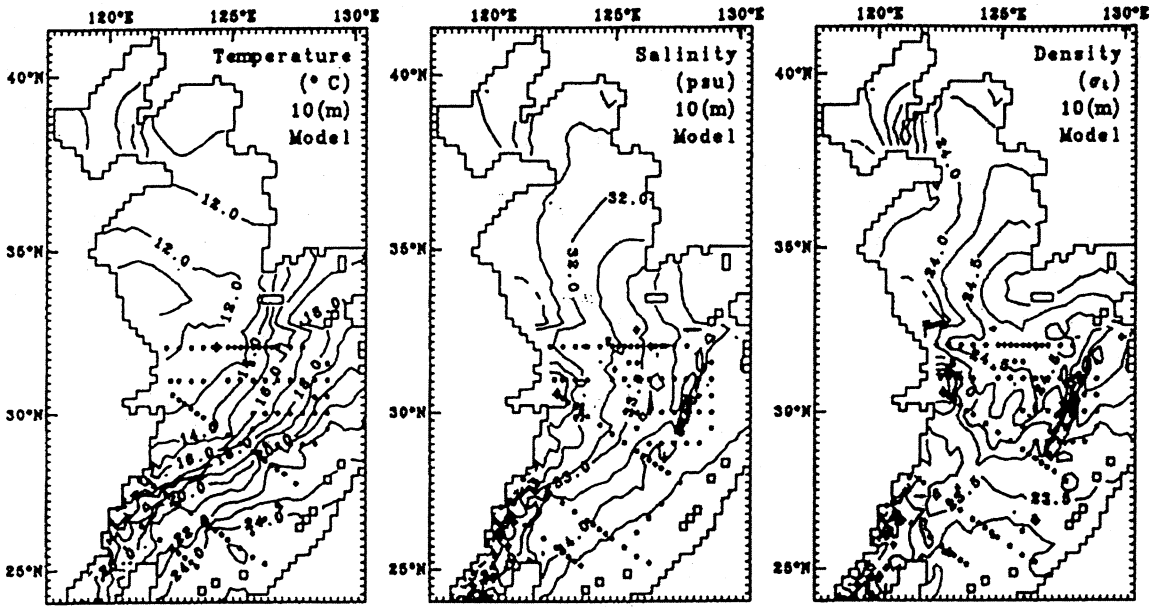

Fig. 1 The water temperature, salinity and density at the depth of 10 m. Black circles denote the observation stations in April 1994.

Given the boundary conditions described later, the above equations are solved by a numerical model (Guo and Yanagi, 1996). The calculation domain is designed to include the ECS, the Yellow Sea and the Bohai Sea (Fig.2). Along the coast of the domain, the six main river discharges (Minjiang, Changjiang, Huanghe, Luanhe, Daliaohe and Yalujiang) are included. The domain is connected to the open ocean by four straits (Taiwan Strait, East of Taiwan, Tokara Strait and Tsushima/Korea Strait) and the volume transports through the four straits are also included in the model. Along the Ryukyu Islands, the domain is closed.

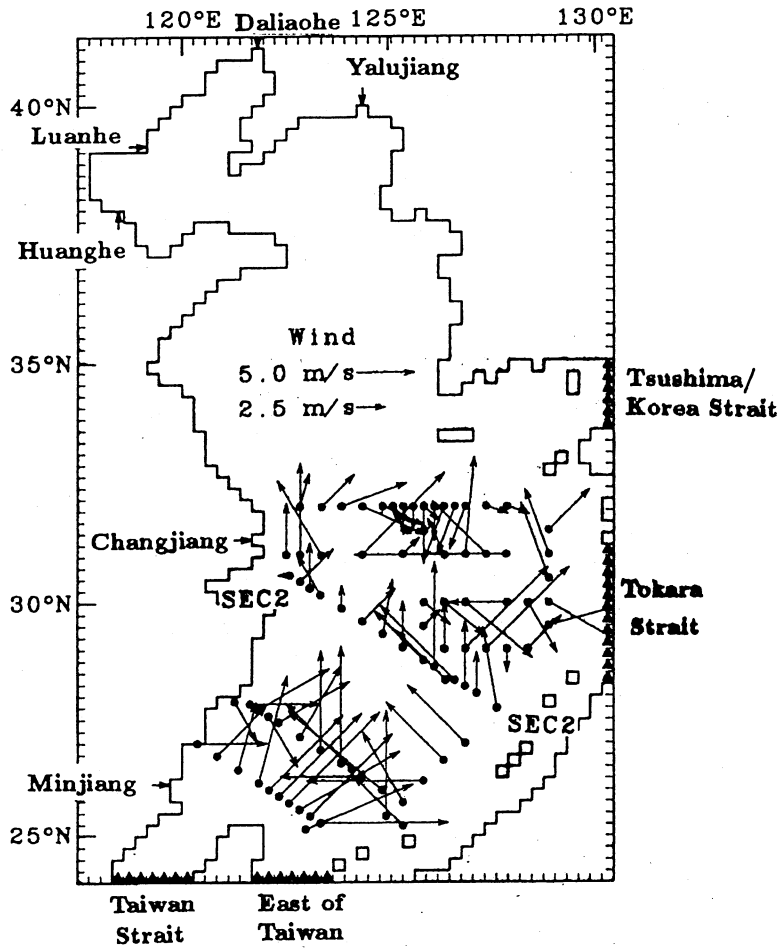

Fig. 2 Wind distribution observed during the observation, that induces an averaged wind of u_a=1 m/s and v_a=2.6 m/s. The open boundaries are denoted by the black triangles and the rivers positions are denoted in the small arrows. 'SEC2' is referred in Figs. 8 and 10.

The river discharges are picked up from Zhang (1996) and the volume transports through the four straits are summarized from many papers (Fang, et al., 1991; Zhao and Fang, 1991; Isobe, 1994; Ichikawa and Beardsley, 1993). Table 1 summarizes these values and some other parameters used in the model, such as the horizontal and vertical resolutions. In these parameters, the horizontal eddy viscosity and diffusivity are related to the amplitude of the M_2 tidal current, based on the mixing length theory (Yanagi, 1996). The vertical eddy viscosity and diffusivity are kept as a constant as they are in Yanagi and Takahashi(1993). The value of γ is also the same as that used in Yanagi and Takahashi(1993).

The boundary conditions of the momentum flux through the sea surface and bottom are:

$$z = 0 : A_v \frac{\partial}{\partial z}(u, v) = \frac{1}{\rho_0}(\tau_x^a, \tau_y^a) \tag{8}$$

$$z = -h : A_v \frac{\partial}{\partial z}(u, v) = \frac{1}{\rho_0}(\tau_x^b, \tau_y^b) \tag{9}$$

where, the wind stresses τ_x^a, τ_y^a and sea bed stresses τ_x^b, τ_y^b are calculated by:

$$(\tau_x^a, \tau_y^a) = \rho_a C_d (u_a, v_a)\sqrt{u_a^2 + v_a^2} \tag{10}$$

$$(\tau_x^b, \tau_y^b) = \rho C_b (u_b, v_b)\sqrt{u_b^2 + v_b^2} \tag{11}$$

Table 1 Parameters, rivers discharge and the volume transports used in the robust diagnostic model.

Definitions	Values		Units	References
	Case 1	Case 2		
Horizontal mesh size	26.5	26.5	km	
Horizontal mesh size	26.5	26.5	km	
Vertical layers	20	20		
Time step	360	360	s	
Horizontal eddy viscosity	10^7	10^7	cm^2/s	YT93
Horizontal eddy diffusivity	10^7	10^7	cm^2/s	YT93
Vertical eddy viscosity	5	5	cm^2/s	YT93
Vertical eddy diffusivity	5	5	cm^2/s	YT93
γ term	1	1	day^{-1}	YT93
Maximum depth	500	500	m	
Minjiang	1700	1700	m^3/s	Zhang(1996)
Changjiang	30000	30000	m^3/s	Zhang(1996)
Huanghe	1300	1300	m^3/s	Zhang(1996)
Luanhe	133	133	m^3/s	Zhang(1996)
Daliaohe	300	300	m^3/s	Zhang(1996)
Yalujiang	1040	1040	m^3/s	Zhang(1996)
Taiwan Strait	1	2	$10^6 m^3/s$	
East of Taiwan	23	23	$10^6 m^3/s$	
Tsushima/Korea Strait	2	2	$10^6 m^3/s$	
Tokara Strait	22	23	$10^6 m^3/s$	

Note: YT93 = Yanagi and Takahashi(1993)

The symbols u_a, and v_a, denote the eastward and northward components of the wind velocity, ρ_a (= 1.2 x 10^{-3}g/cm^3) is the density of air, C_d (= 1.3 x 10^{-3}) is the non-dimensional drag coefficient at the surface, u_b and v_b are the velocities above the sea bed, and C_b (= 2.6 x 10^{-3}) is the drag coefficient at the sea bed.

The raw wind data at all observation stations recorded by the ship show a large variation (Fig.2). Considering a one month time scale, we use the mean wind during the observation period (u_a = 1.0 m/s and v_a = 2.6 m/s) in the diagnostic calculation.

FLOW FIELD

The total kinetic energy at all grids was used to check if the calculation reaches a steady state. After 15 days' calculation, the kinetic energy approaches a steady state. However, the calculation was last for 30 days finally.

The calculated residual currents at 10 m in the two cases and their difference are shown in Fig.3. Compared to the schematic flow pattern (Fig. 4, Guan, 1994), the reproduced currents in the two cases both represent the main characteristics of the current system in the ECS. Since a detailed description about the calculated current in Case 1 may be found in Guo et al. (1997), we focus on the difference between these two cases here.

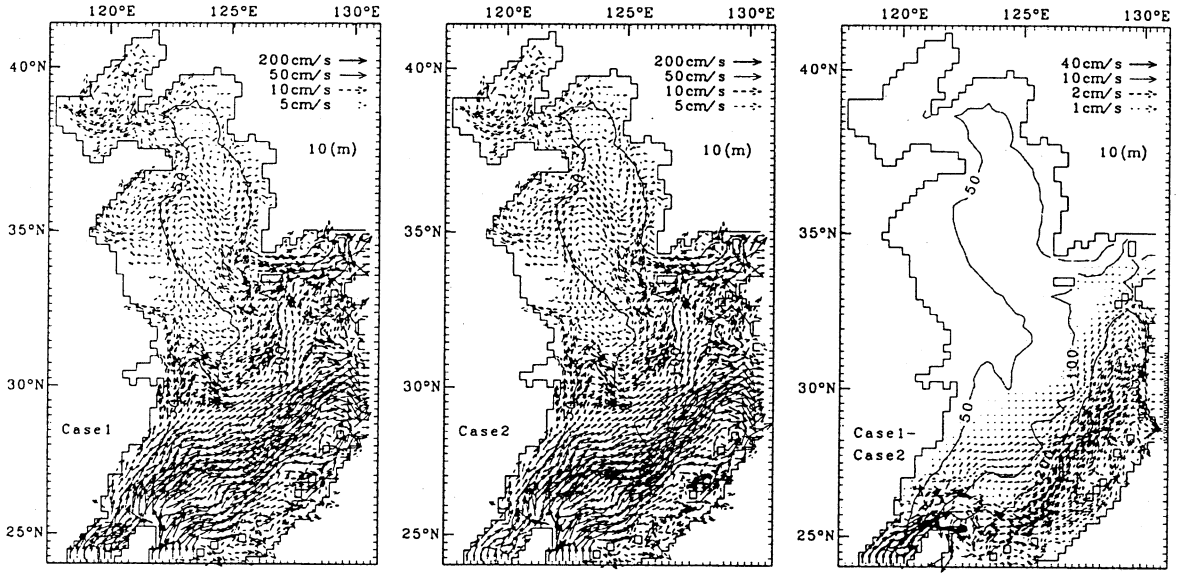

Fig. 3 Calculated residual currents at the depth of 10 m in the two cases and their difference. The lines in the vector field are the contours of the depths of 50 m, 100 m and 200 m.

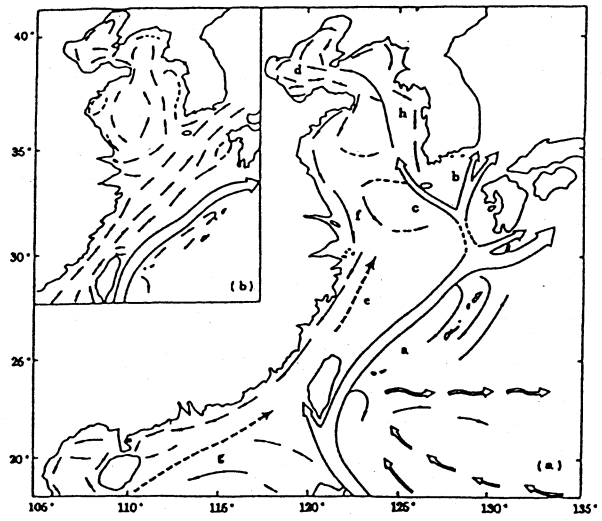

Fig. 4 Schematic representations of the major current systems in the Bohai, Yellow Sea and East China Sea for winter(a) and summer(b) (after Guan, 1994).

Because the volume transport through the East of Taiwan and Tsushima/Korea Strait are fixed in the two cases, the difference between the two cases is that 1 Sv water flows into the ECS from the Taiwan Strait and flows out from the Tokara Strait. Figure 3 clearly shows such a current system, that is, the water enters into the domain from the Taiwan Strait, then flows along the continental slope, finally exiting out from the Tokara Strait.

CHEMICAL-BIOLOGICAL PROCESSES

NUMERICAL MODEL AND PARAMETERS

Five compartments (DIN, DIP, phytoplankton, zooplankton and detritus) are incorporated in an ecological numerical model as shown in Fig.5 and the equations controlling these compartments are:

Phytoplankton(P):

$$\frac{\partial P}{\partial t} + \vec{u}\cdot\nabla P + S_p\frac{\partial P}{\partial z} = DIF(P) + A_1P - A_2P^2 - A_3Z \qquad (12)$$

Zooplankton(Z):

$$\frac{\partial Z}{\partial t} + \vec{u}\cdot\nabla Z = DIF(Z) + A_3Z - A_4Z^2 - A_5Z - A_6Z \qquad (13)$$

Detritus(D):

$$\frac{\partial D}{\partial t} + \vec{u}\cdot\nabla D + S_d\frac{\partial D}{\partial z} = DIF(D) + A_2P^2 + A_4Z^2 + A_5Z - A_7D \qquad (14)$$

DIN(N_N):

$$\frac{\partial N_N}{\partial t} + \vec{u} \cdot \nabla N_N = DIF(N_N) - A_1 P + A_6 Z + A_7 D \tag{15}$$

DIP(N_P):

$$\frac{\partial N_P}{\partial t} + \vec{u} \cdot \nabla N_P = DIF(N_P) - A_1 P + A_6 Z + A_7 D \tag{16}$$

where

$$DIF(\,) = \frac{\partial}{\partial x}\left(K_h \frac{\partial}{\partial x}\right) + \frac{\partial}{\partial y}\left(K_h \frac{\partial}{\partial y}\right) + \frac{\partial}{\partial z}\left(K_v \frac{\partial}{\partial z}\right);$$

The meanings of the biochemical terms in above equations are as follows.

- A_1P: Photosynthesis of phytoplankton in which the growth rate A_1 is decided by:

$$A_1 = V_m \min\{V_1(N_N), V_1(N_P)\}\, V_2(I)\, V_3(T)\, V_4(S) \tag{17}$$

$$V_1(N_N) = \frac{N_N}{K_{SN} + N_N} \tag{18}$$

$$V_1(N_P) = \frac{N_P}{K_{SP} + N_P} \tag{19}$$

$$V_2(I) = \frac{I}{I_{opt}} \exp\left(1 - \frac{I}{I_{opt}}\right) \tag{20}$$

$$V_3(T) = \frac{T}{T_{opt}} \exp\left(1 - \frac{T}{T_{opt}}\right) \tag{21}$$

$$V_4(S) = \frac{S}{S_{opt}} \exp\left(1 - \frac{S}{S_{opt}}\right) \tag{22}$$

where V_m denotes the maximum photosynthetic rate of phytoplankton, K_{SN} and K_{SP} the half saturation constant for DIN and DIP uptake, respectively, T_{opt} and S_{opt} the optimum water temperature and salinity for the growth of phytoplankton, respectively, I the light intensity and I_{opt} the optimum light intensity for the growth of phytoplankton. The light intensity I in the water is expressed as:

$$I(z) = I_s \exp\left[-\int_0^z k(z)dz\right] \tag{23}$$

$$k(z) = 0.04 + 0.054C(z)^{\frac{2}{3}} + 0.0088C(z) \tag{24}$$

$$C(z) = P(z) + \delta(Z(z) + D(z)) \tag{25}$$

where, I_s denotes the light intensity at the sea surface, k the extinction coefficient, C the concentration of chlorophyll *a*. The self-shading of phytoplankton is represented by Eq.(24) (Riley, 1956) and the zooplankton and detritus are included in this effect vis Eq.(25), in which δ is a parameter to consider the different contribution of the zooplankton and detritus from the phytoplankton.

- A_2P^2: Natural mortality of phytoplankton. A_2 is set to a constant.
- A_3Z: Grazing of zooplankton. A_3 is expressed by:

$$A_3 = R_{max}[1 - \exp\lambda(-P + P^*)] \tag{26}$$

where R_{max} denotes the maximum grazing rate, λ the Ivlev constant, P* the Threshold of phytoplankton concentration for possible grazing by zooplankton. When P is smaller than P*, A_3 is set to zero.

- A_4Z^2: Natural mortality of zooplankton. A_4 is set to a constant.
- A_5Z: Egestion of zooplankton. The production rate of fecal pellets of zooplankton, A_5, is given by:

$$A_5 = \iota R_{max}[1 - \exp\lambda(-P + P^*)] \tag{27}$$

where ι (= 0.2) is the ratio of fecal pellets production to the predation.

- A_6Z: Excretion of zooplankton. The generation rate of urine of zooplankton, A_6, is set to a constant.
- A_7Z: Decomposition of detritus. The decomposition rate of detritus, A_7 is set to a constant.
- $S_p\partial P/\partial z$: Sinking of phytoplankton. The sinking velocity of phytoplankton is set to a constant.
- $S_d\partial D/\partial z$: Sinking of detritus. The sinking velocity of detritus is set to a constant.

In Table 2, we present the parameters used in the ecological numerical model with their references. Because there are few observed data about such parameters in the ECS, we have to refer them to the observed data in other regions or the values used in other ecological models. Some of them are determined as their use makes the calculated results approach the observed data. Thus some parameters are denoted as 'guess' in Table 2. In addition to these parameters, the

horizontal and vertical eddy diffusivities are the same as those used in the robust diagnostic model for the residual current.

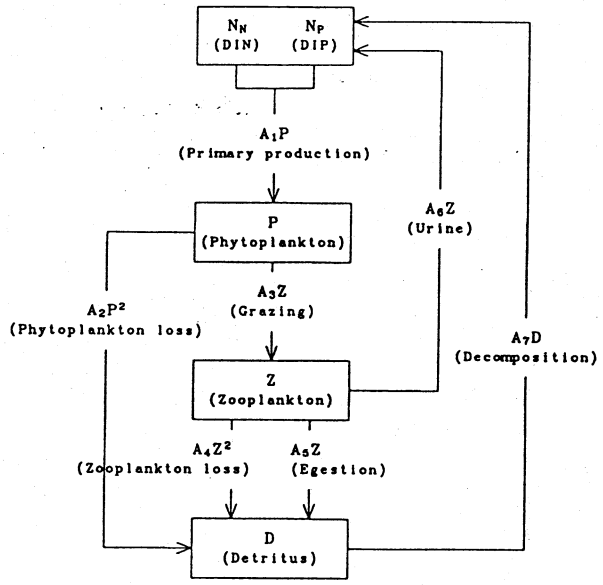

Fig. 5 Components of the ecological model.

We consider that the nutrients (DIN and DIP) in the region shallower than 200 m in the ECS has three sources, that are the rivers (mainly Changjiang and denoted as DINC and DIPC), the Taiwan Strait (DINT and DIPT) and the shelf edge (DINK and DIPK). To estimate the contributions of the above three sources of DIN and DIP in the ECS, we labeled them in the model, which means the model solves three similar equations for the three sources of DIN and DIP, respectively.

The advective and diffusion terms in Eqs. (15) and (16) may be separated linearly. The difficulty is the separation of the nonlinear biochemical terms. We implement this separation based on the content ratio of the three sources of DIN and DIP in a grid. For example, the biochemical terms for DINC and DIPC are expressed as

$$\frac{DINC}{DINC + DINT + DINK} \times (-A_1P + A_6Z + A_7D) \quad (28)$$

and

$$\frac{DIPC}{DIPC + DIPT + DIPK} \times (-A_1P + A_6Z + A_7D), \quad (29)$$

respectively. The equations for the other two sources of nutrients are obtained in a similar way.

In order to distinguish the different sources of nutrients in the model, we set zero concentration as the initial condition of all compartments. This condition leads to a long computer time but has to be kept because we do not know the ratio of different sources of nutrients in a given initial field.

Table 2 Parameters and their references used in the ecological model.

Definitions	Symbol	Values	Units	References
Horizontal mesh size		26.5	km	
Horizontal mesh size		26.5	km	
Vertical layers		20		
Time step		3600	s	
Maximum depth		500	m	
Sinking velocity of phytoplankton	S_p	33	cm/day	Smayda(1970)
Singing velocity of detritus	S_d	100	cm/day	Nakata(1993)
Maximum photosynthetic rate	V_m	2.0	day^{-1}	Eppley(1972)
Half saturation constant for DIN	K_{SN}	3.0	$mmol/m^3$	Kawamiya et al.(1995)
Half saturation constant for DIP	K_{SP}	0.1	$mmol/m^3$	Guess
Optimum light intensity for phytoplankton	I_{opt}	150	$cal/cm^2/day$	Eppley, et al.(1969)
Light intensity on sea surface	I_s	350	$cal/cm^2/day$	Observation
Optimum temperature for phytoplankton	T_{opt}	25	°C	Yamaguchi(1991)
Optimum salinity for phytoplankton	S_{opt}	30	psu	Yamaguchi(1991)
Natural mortality rate of phytoplankton	A_2	0.05	$(mgN/m^3 \cdot day)^{-1}$	Guess
Maximum grazing rate of zooplankton	R_{max}	1.5	day^{-1}	Uye and Yashiro(1988)
Ivlev constant	λ	0.47	$(mgChl.a/m^3)^{-1}$	Smayda(1973)
Threshold of phytoplankton in grazing	P^*	0.1	$mgChl.a/m^3$	Guess
Natural mortality rate of zooplankton	A_4	0.05	$(mgN/m^3 \cdot day)^{-1}$	Guess
Fecal pellet coefficient of zooplankton	ι	0.2		Butler et al.(1969)
Urine coefficient of zooplankton	A_6	0.1	day^{-1}	Guess
Bacterial decomposition rate of detritus	A_7	0.05	day^{-1}	Fasham et al.(1990)
DIP:Chlorophyll a		21:16		Yamada et al.(1994)

The ecological model has the same four open boundaries as the residual current model (Fig.2). By extrapolation of the observed data, the boundary conditions are decided (Guo et al., 1997), except for the zooplankton, which was not included in the observation in April, 1994. A general zooplankton biomass data in the ECS (wet weight, 50 - 100 mg/m^3, Hattori and Motoda, 1983) are kept along the open boundary.

The major features of nutrient elements in large Chinese rivers were summarized by Zhang (1996). In our model, the concentrations of DIN and DIP and the fresh water discharges presented by Zhang (1996) are used for calculating the nutrients' input from the rivers. As for the phytoplankton, zooplankton and detritus, no input from rivers is assumed.

The fluxes of five compartments through the sea surface and bottom are assumed to be zero,

except for the flux of the detritus through the sea bottom, where the sedimentation rate (2mgN/m^2/day, Oguri et al., 1997) is used.

CALCULATED RESULTS

The above model has been used to reproduce the observed DIN, DIP, phytoplankton and detritus in April 1994, using the flow field of the Case1 in Fig.3 (Guo et al., 1997, hereafter referred as Case1). The horizontal and vertical distributions of the calculated results are very similar to the observed data, except for some small structure. Figure 6 shows the direct comparison between the calculated results and the observed data. Generally, the model may be accepted to reproduce the observed results well.

Changing the flow field to that of the Case2 in Fig.3, the ecological model is run again, using the same parameters and boundary conditions as in Case1. The horizontal distribution of the five compartments at 10 m in these two cases are shown in Fig.7 (a) and (b), respectively. In the ECS, with the change of the volume transport through the Taiwan Strait, DIP and detritus changed largely, while DIN, phytoplankton and zooplankton change little.

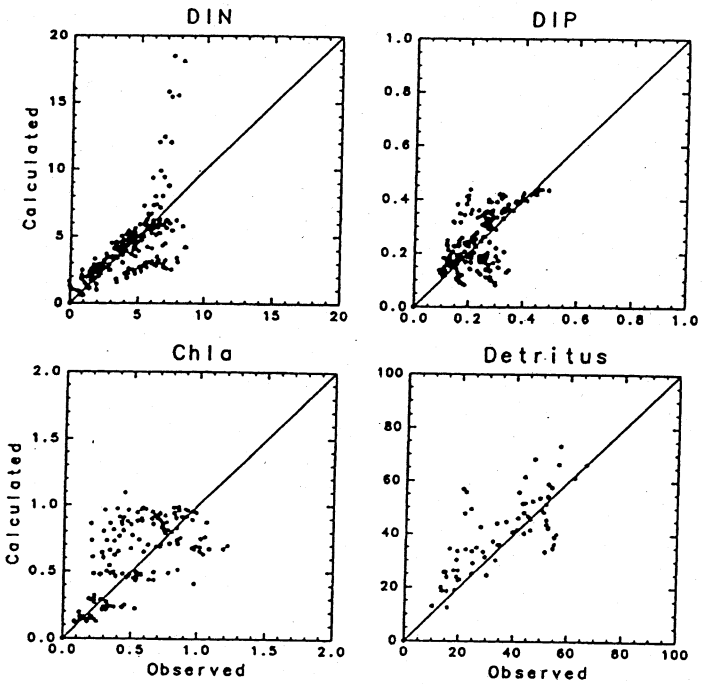

Fig. 6 Comparison of the calculated results with the observed data. X-axis represent the observed data, Y-axis the calculated results.

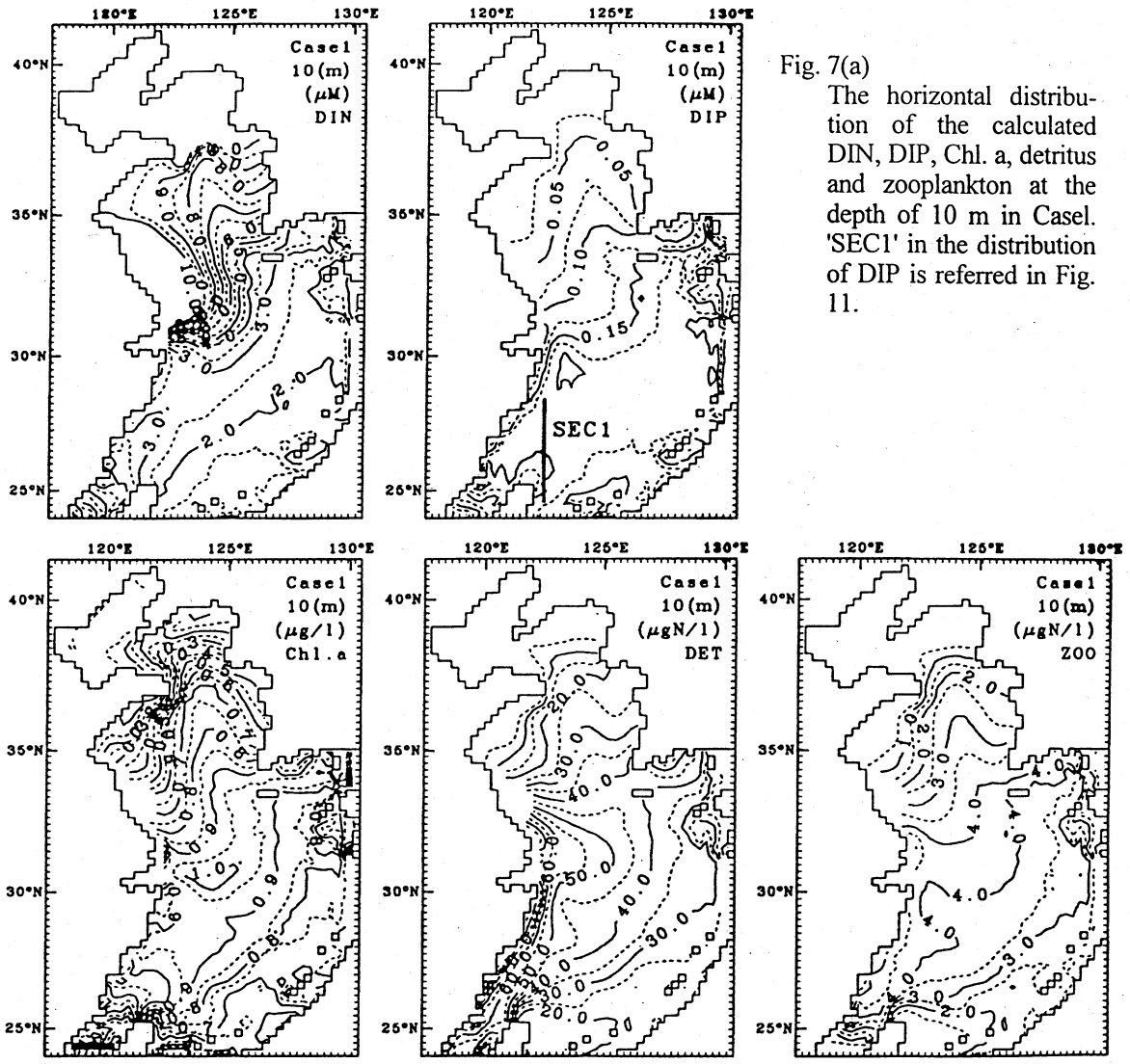

Fig. 7(a)
The horizontal distribution of the calculated DIN, DIP, Chl. a, detritus and zooplankton at the depth of 10 m in Casel. 'SEC1' in the distribution of DIP is referred in Fig. 11.

Physically, the decrease of the volume transport through the Taiwan Strait will reduce the input of the five compartments into the ECS from the Taiwan Strait. Meanwhile, the intrusion of the Kuroshio water into the ECS from the East of Taiwan will be strengthened, that will compensate the decrease in the Taiwan Strait somewhat. However, this compensation will depend on the concentration difference of the compartments in the Taiwan Strait and the East of Taiwan largely.

The decrease of the detritus in the ECS may be explained by its high concentration in the

Taiwan Strait and low concentration in the East of Taiwan. The increase of the DIP in the ECS is caused by the intrusion of the Kuroshio water clearly. The reasons for the little change in the DIN, phytoplankton and zooplankton are considered as that the concentration difference is little. In fact, the input of the phytoplankton and zooplankton from the boundary just shares a little part in their standing stocks in the ECS. Most of them are produced by the primary and second production in the ECS.

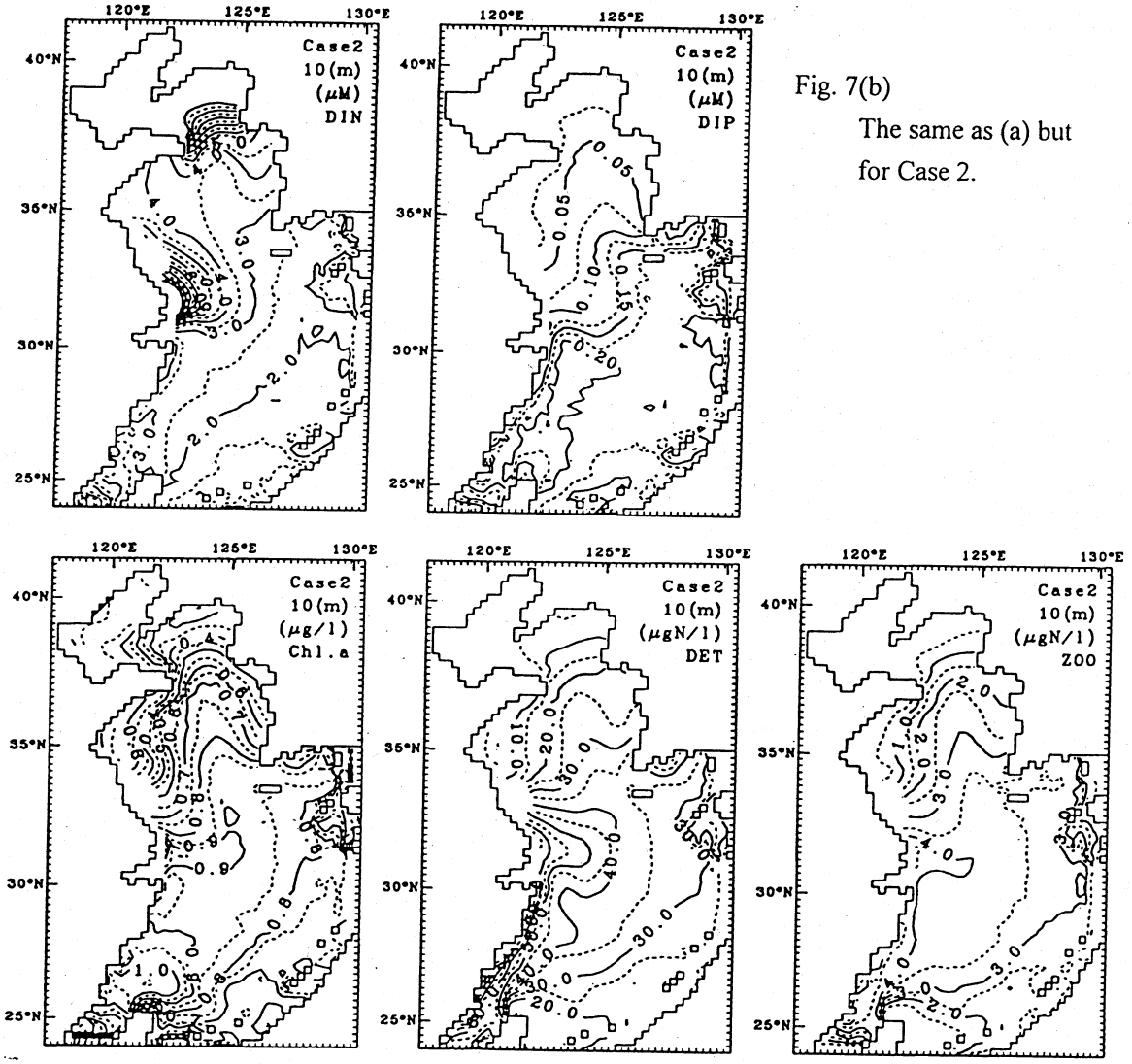

Fig. 7(b)
The same as (a) but for Case 2.

The vertical distribution of the five compartments along a transect (SEC2 in Fig.2), calculated

in the two cases are shown in Fig.8 (a) and (b), respectively. This transect has nearly the same location, with the PN line observed regularly by the Nagasaki Marine Observatory, Japan. The general vertical structures of these compartments are reproduced well in both cases. However, due to the distance from the transect to the south boundary, little change may be found in these two cases, except for the detritus.

As described in the last section, the nutrients in the ECS are thought to come from three sources, that are the rivers, the Taiwan Strait and the shelf edge. Because the input of the nutrients from the rivers is the same in the two cases of model run, we only present the horizontal and vertical distribution of the nutrients from the Taiwan Strait and the shelf edge in Figs. 9, 10 and 11.

From Fig.9, we can know that with the change of the volume transport through the Taiwan Strait, the concentration of the DINT and DIPT in the ECS decrease largely, and their influenced region becomes small. Meanwhile, the high concentration region of the DINK and DIPK spread throughout the ECS. Thus the total DIN or DIP are maintained.

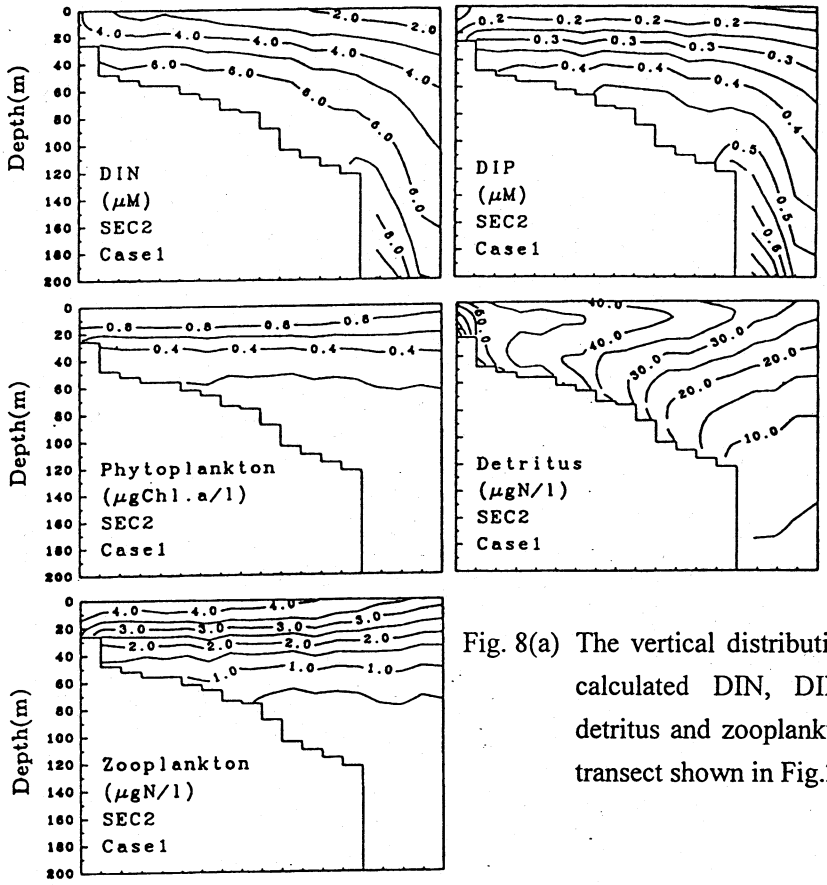

Fig. 8(a) The vertical distribution of the calculated DIN, DIP, Chl.a, detritus and zooplankton at the transect shown in Fig.2.

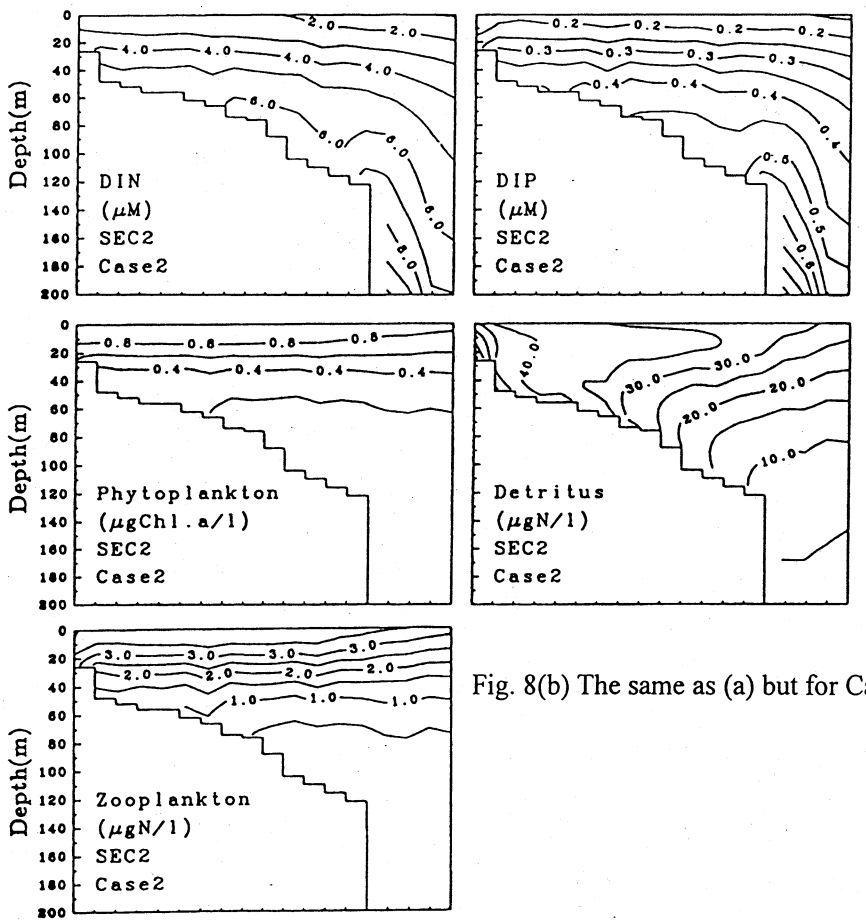

Fig. 8(b) The same as (a) but for Case 2.

Figure 10 may clearly illustrate to us the mechanism on the above compensation process. The DINT and DIPT exist mainly in the upper layer and the decrease also occurs in the upper layer. However the DINK and DIPK have a high concentration in the deep water, especially in the shelf edge. The upwelling of Kuroshio water in the shelf edge supplies a large mount of DIN and DIP into the continental shelf of the ECS. With the decrease of the volume transport through the Taiwan Strait, the upwelling of Kuroshio water is strengthened. Therefore the concentrations of DINK and DIPK along the transect become high, especially in the deep layer.

This process may be further confirmed by Fig.ll, in which the nutrients' distribution along SEC1 (see Fig.7(a) for its position) is shown. Clearly, near the shelf edge, the DINK and DIPK are increased by the upwelling there induced by the change of the volume transport through the Taiwan Strait. The distributions of the DINT and DIPT are interesting. Because of their shallow sources and the upwelling near the shelf edge, a low concentration may be found near the bottom.

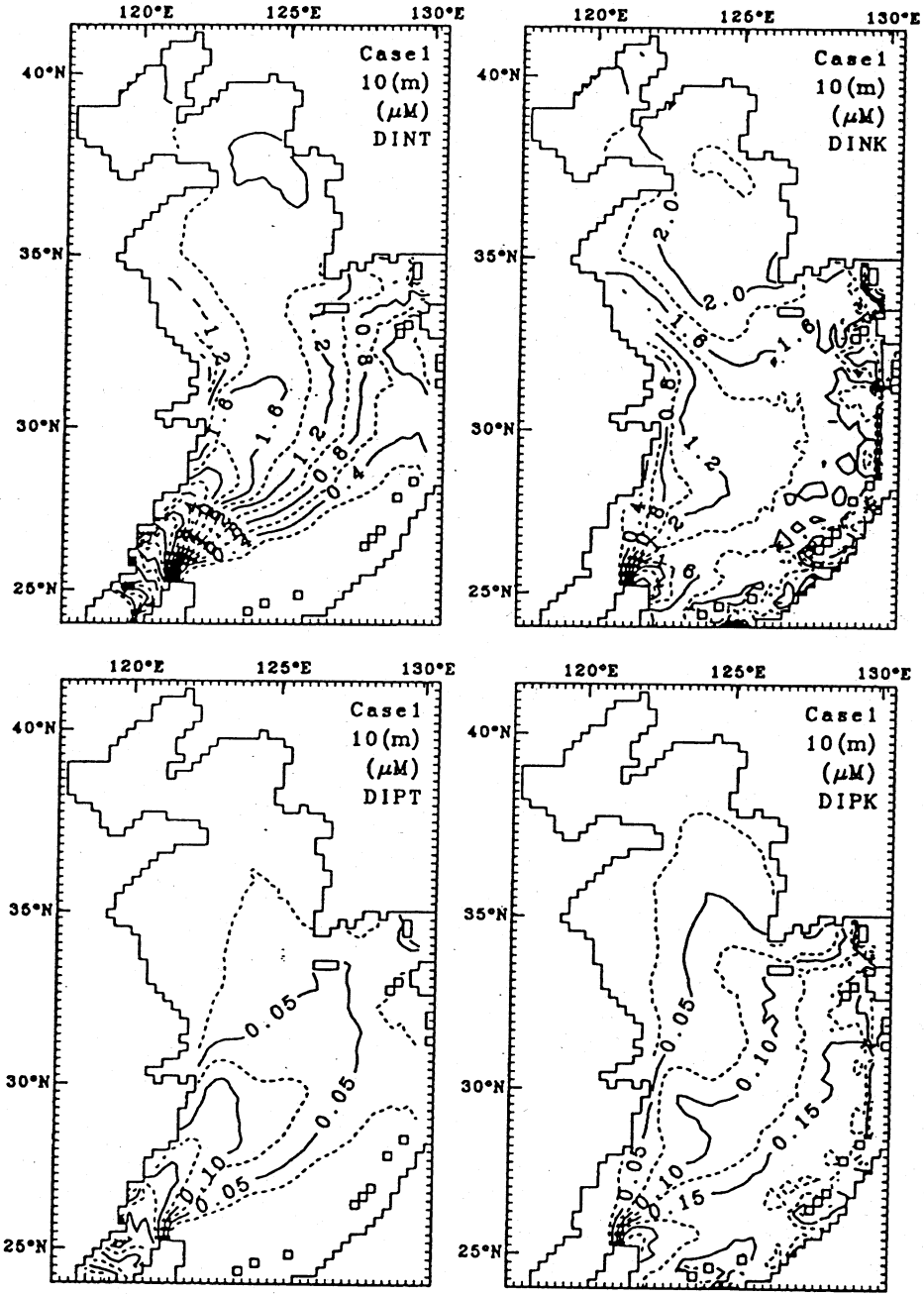

Fig. 9(a) Horizontal distribution of the DIN and DIP supplied from the Taiwan Strait (DINT and DIPT) and the shelf edge (DINK and DIPK) at the depth of 10 m.

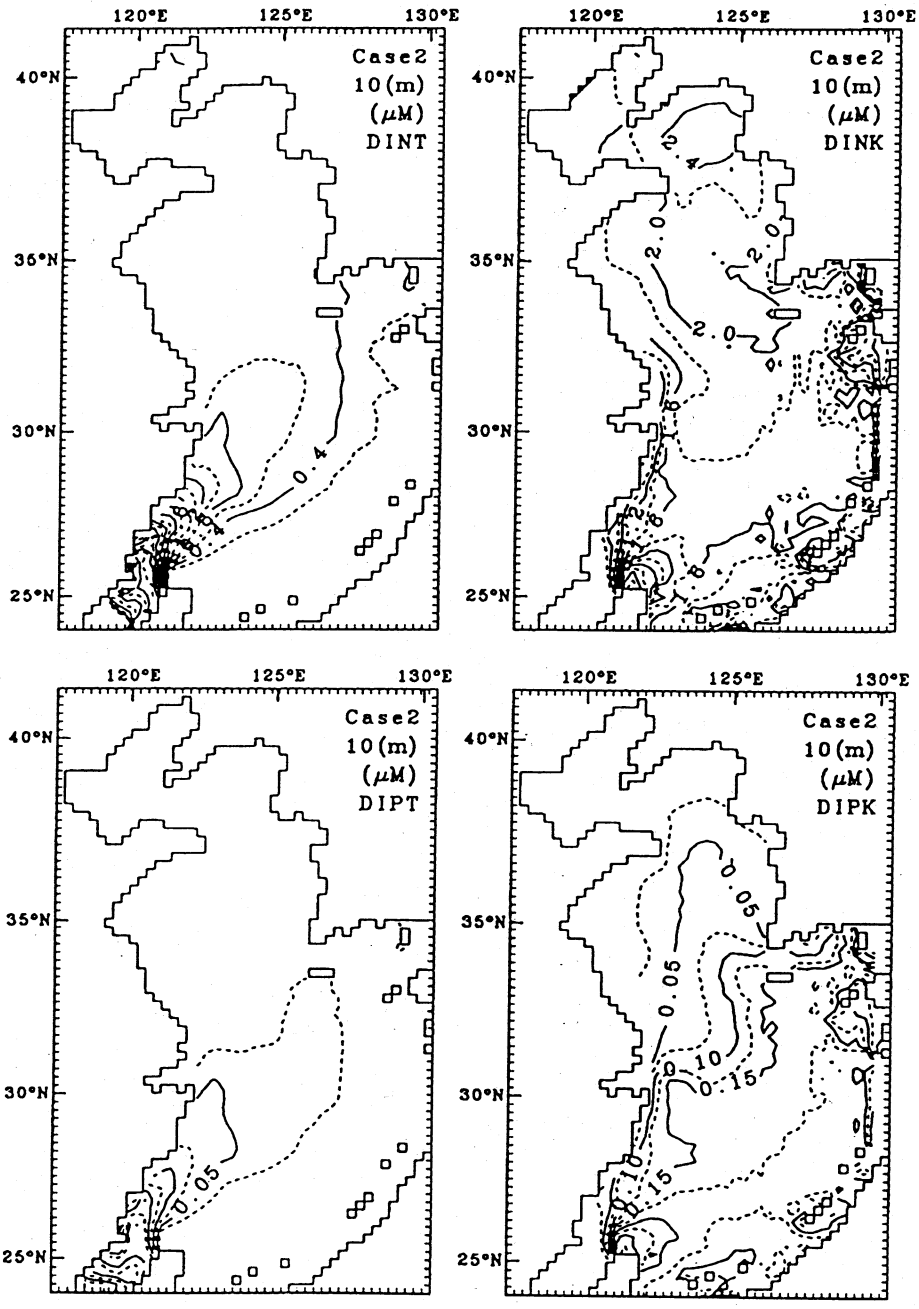

Fig. 9(b) The same as (a) but for Case 2.

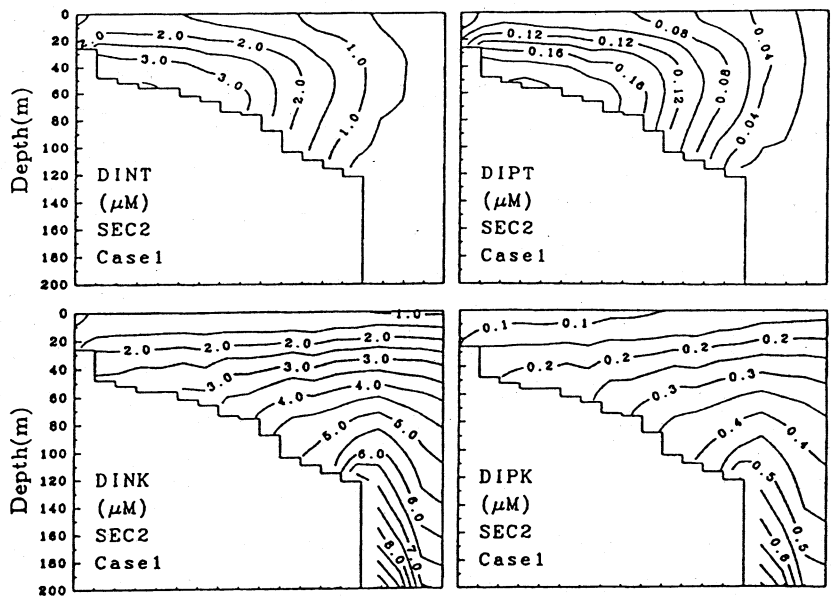

Fig. 10(a) Vertical distribution of the DIN and DIP supplied from the Taiwan Strait (DINT and DIPT) and the shelf edge(DINK and DIPK) at a transect (SEC2 in Fig. 2).

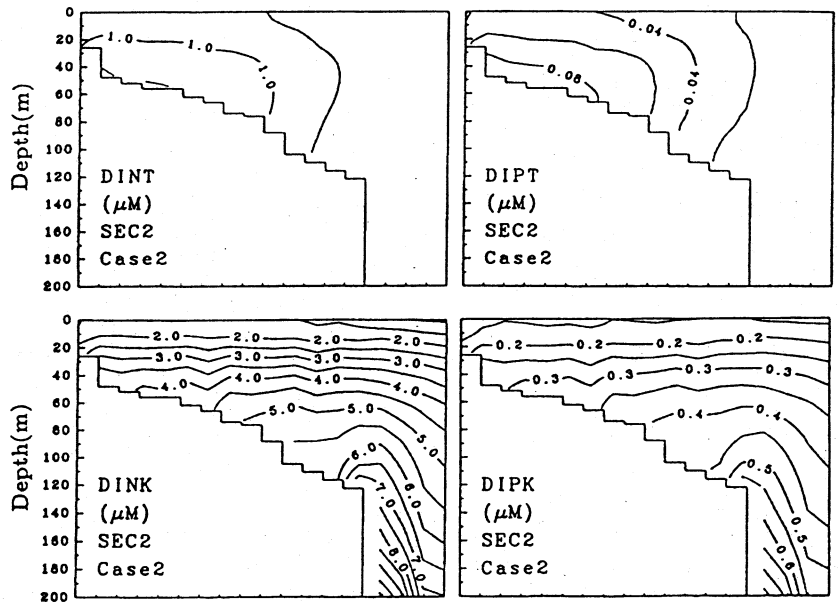

Fig. 10(b) The same as (a) but for Case 2.

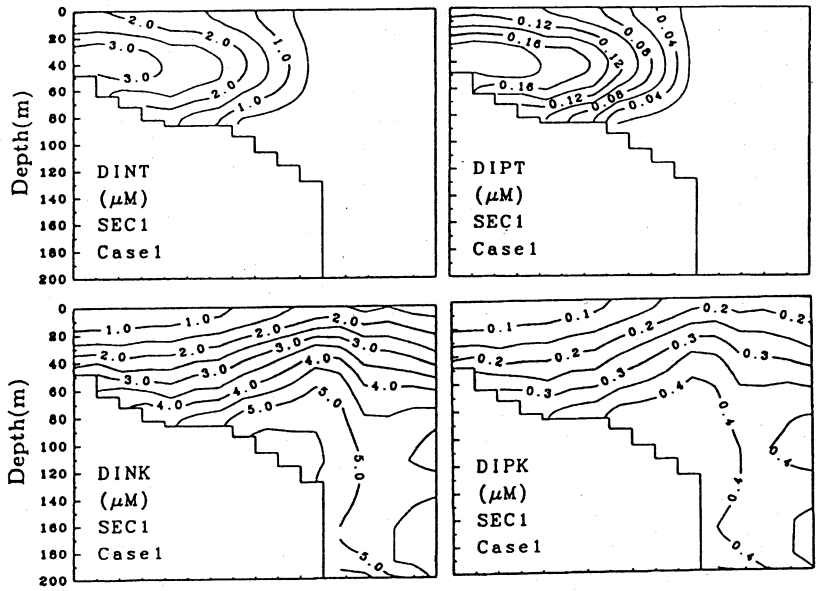

Fig. 11(a) Vertical distribution of the DIN and DIP supplied from the Taiwan Strait (DINT and DIPT) and the shelf edge(DINK and DIPK) at a transect (SEC1 in Fig.7(a)).

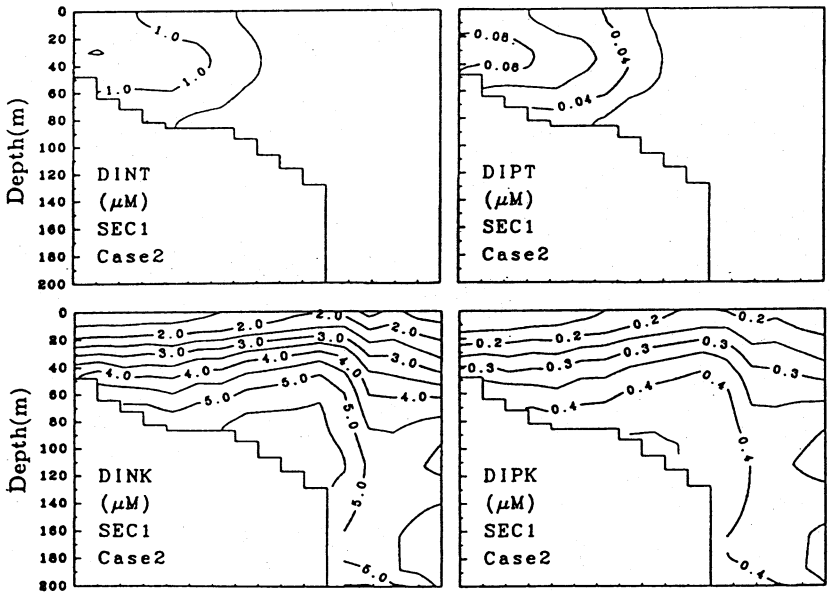

Fig. 11(b) The same as (a) but for Case 2.

DISCUSSIONS

The above results suggest that the change of the volume transport through the Taiwan Strait has little influence on the primary production in the ECS. This is because the decrease of the nutrients input from the Taiwan Strait may be compensated by the nutrients input from the shelf edge. However, it must be noted that if the variation happens to the concentrations of the DIN or DIP in the Taiwan Strait, not the volume transport through it, the compensation process will take no effect.

In the calculation of the current, the density structures in the two cases are basically the same due to the use of a robust diagnostic model. Thus the change of baroclinic current is not considered. To clarify its influence on our conclusion, we present the depth-averaged current calculated by Case 1 in Fig.12. Compared to Fig.3, we can know the current in the ECS is mainly controlled by the barotropic current. Moreover, the kinetic energy from the barotropic current and baroclinic current are calculated respectively and their ratio is 10:3 in the domain. Thus the exclusion of the change of baroclinic current will have little influence on our conclusion.

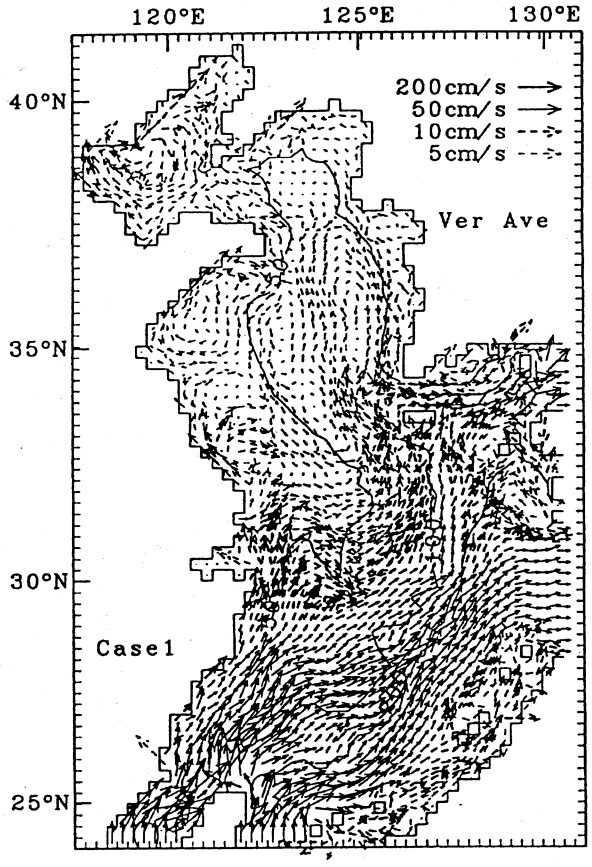

Fig.12 Horizontal distribution of the vertical averaged current calculated by Case 1

From the viewpoint of the material transport, it is important to clarify the different roles of the nutrients from the rivers, the Taiwan Strait and the shelf edge in the ecosystem of the ECS. But as shown in this paper, the physical factor greatly influences their roles. If a small volume transport is assumed to pass through the Taiwan Strait, the nutrients supplied from the Kuroshio water will increase naturally, like that discussed in Chen and Wang (1997). So before calculating the nutrients budget in the ECS, we must clarify the volume transports through the four straits in the ECS and their variations at first.

Considering the difficulties and the costs of the long period observation, we plan to solve this problem by using a regional high resolution numerical model that is nested in the Pacific ocean model. This model is now being developed and its results will be reported in the next PAMS-JECSS workshop.

ACKNOWLEDGMENTS

The authors express their sincere thanks to the Chinese scientists who took part in the observation in April 1994. The authors are also grateful to Prof. H. Takeoka of Ehime University for his helpful suggestions about this research. The 'DENNOU' graphic library was used to draw the figures. This study is partly sponsored by the Science and Technology Agency of Japan.

REFERENCES

Baretta, J. W. and P. Raurdij (1988) *Tidal fiat estuaries.* Springer-Verlag, 353 pp.

Butler, E. I., E. D. S. Corner and S.M. Marshall (1969) On the nutrition and metabolism of zooplankton VI. Feeding efficiency of Calanus in terms of nitrogen and phosphorus. *J. Mar. Biol. Assoc. U.K.*, **49**, 977-1001.

Chen, C. T. A. and S. L. Wang (1997) Carbon and nutrient budgets on the East China Sea continental shelf. in *Biogeochemical Processes in the North Pacific*, S. Tsunogai, ed., 169-186.

Eppley, R. W. (1972) Temperature and phytoplankton growth in the sea. *Fish. Bull. US*, **70**, 1063-1085.

Eppley, R. W., J. N. Rogers and J. J. McCarthy (1969) Half saturation constants for uptake of nitrate and ammonium by marine phytoplankton. *Limnol. Oceanogr.*, **14**, 912-920.

Fang, G., B. Zhao and Y. Zhu (1991) Water volume transport through the Taiwan Strait and the continental shelf of the East China Sea measured with current meters. in *Oceanography of Asian Marginal Seas*, K. Takano, ed., Elsevier, 345-358.

Fasham, M.J.R., H.W. Ducklow and S.M. McKelvie (1990) A nitrogen-based model of plankton dynamics in the oceanic mixed layer. *J. Mar. Res.*, **48**, 591-639.

Fu Z., J. Hu and G. Yu (1990) Sea water flux through Taiwan Strait. *Chin. J. Oceanol. Limnol.*, **9**,

232-239.

Fujio, S. and N. Imasato (1991) Diagnostic calculation for circulation and water mass movement in the deep Pacific. *J. Geophys. Res.*, **96**, 759-774.

Guan, B. (1994) Patterns and structures of the currents in Bohai, Huanghai and East China Seas. in *Oceanology of China Seas, Vol. 1*, D. Zhou, Y. Liang and C. Zeng, eds, Kluwer Academic Publishers, Netherlands, 17-26.

Guo, X. and T. Yanagi (1996) Seasonal variation of residual current in Tokyo Bay, Japan - diagnostic numerical experiments. *J. Oceanogr.*, **52**, 597-616.

Guo, X. and T. Yanagi (1997) Three dimensional structure of tidal currents in the East China Sea. *J. Oceanogr.* (in press).

Guo, X., T. Yanagi and D. Hu (1997) Ecological modeling in the East China Sea. *J. Mar. Res.* (submitted).

Hattori, H. and S. Motoda (1983) Regional difference in zooplankton communities in the Western North Pacific Ocean (CSK Data). *Bull. Plankton Soc., Japan*, **30**, 53-63.

Ichikawa, H. and R. C. Beardsley (1993) Temporal and spatial variability of volume transport of the Kuroshio in the East China Sea. *Deep-Sea Res.*, **40**, 583-605.

Isobe, A (1994) Seasonal Variability of the barotropic and baroclinic motion in the Tsushima/Korea Straits. *J. Oceanogr.*, **50**, 223-238.

Isobe, A. (1997) On the origin of the Tsushima Warm Current and its seasonality. *Cont. Shelf. Res.* (Accepted)

Kawamiya M., M.J. Kishi, Y. Yamanaka and N. Suginohara (1995) An ecological-physical coupled model applied to Station papa. *J. Oceanogr.*, **51**, 635-664.

Kishi, M.J. and S. Ikeda (1986) Population dynamics of "red tide" organisms in eutrophicated coastal water - numerical experiment of phytoplankton bloom in the East Seto Inland Sea, Japan. *Ecol. Model.*, **31**, 145-174.

Kremer, J. H. and S. W. Nixon (1978) A coastal marine ecosystem: Simulation and analysis, in *Ecological Studies*, **24**, Springer Verlag, 217pp.

Nakata, K (1993) Ecosystem Model: its formulation and estimation method for unknown rate parameters. *J. Adv. Mar. Tech. Conf.*, **8**, 99-138 (in Japanese with English abstract and captions).

Oguri, K., E. Matsumoto, Y. Saito, T. Hama, M. Yamada, H. Narita and K. Iseki (1997) Rates of sediment accumulation and carbon burial measured with ^{210}Pb in the East China Sea. in Biogeochemical Processes in the North Pacific, S. Tsunogai ed., *Japan Marine Science Foundation*, Tokyo, Japan, 360-367.

Riley, G. A. (1956) Oceanography of Long Island Sound, 1952-1954, II. Phys. Oceanogr. *Bull. Bing. Ocean. Coll.* **15**, 15-46.

Sarmiento, J. L. and K. Bryan (1982) An ocean transport model for the North Atlantic. *J. Geophys. Res.*, **87**, 394-408.

Smayda, T. J (1970) The suspension and sinking of phytoplankton in the sea. *Oceanogr. Mar.*

Biol. Ann. Rev., **8**, 353-414.

Smayda, T. J. (1973) The growth of Skeletonema costatum during a winter-spring bloom in Narragansett Bay. *R. I. Norw. J. Bot.*, **20**, 219-247.

Steele, J. H (1974) *The structure of marine ecosystems*. Cambridge, Mass., Harvard University Press, 1-128.

Uye, S. and M. Yashiro (1988) Respiration rates of planktonic crustaceans from the Inland Sea of Japan with special reference to the effects of body weight and temperature. *J. Oceanogr.*, **44**, 47-51.

Yamaguchi, M (1991) The growth characteristics of diatom. in *Report of ecological measure for the toxic red tide*, Nansei National Fisheries Institute, 55-66 (in Japanese).

Yamada M., K. Makihara and S. Montani (1994) Nutrients environment influencing the distribution of phytoplankton in Dokai Bay, Japan. *Abstracts on the spring Conference of Oceanographic Soc. of Japan*, 335-336 (in Japanese).

Yanagi T. (1996) Material exchange processes at the shelf edge. *Umi no Kenkyu (Research in Oceanography)*, **5**, 25-34 (in Japanese).

Yanagi, T. and S. Takahashi (1993) Seasonal variation of circulations in the East China Sea and the Yellow Sea. *J. Oceanogr.*, **49**, 503-520.

Yanagi, T., K. Inoue, S. Montani and M. Yamada (1997) Ecological modeling as a tool for coastal zone management in Dokai Bay, Japan. *J. Mar. Syst.*, **13**, 123-136.

Zhang, J. (1996) Nutrient elements in large Chinese estuaries. *Cont. Shelf Res.*, **16**, 1023-1045.

Zhao, B. and G. Fang (1991) Estimation of water volume transport through the main straits of the East China Sea. *Acta Oceanologica Sinica*, **10**, 1-13.

台灣海洋學刊　　第37期 第2號,139-164頁,2表,12圖, 中華民國87年9月

東海生態模式中臺灣海峽的作用

郭新宇[1]、柳哲雄[2]

(received 1998/2/17, revised 1998/5/8, accepted 1998/5/18)

摘　要

利用 1994 年 4 月的東海海洋觀測資料，我們開發了一個包括溶解性無機氮(DIN)，溶解性無機磷(DIP)，浮游植物、浮游動物，及碎屑(detritus)等五個變量的東海生態模式，在基本再現了觀測資料的基礎上，通過改變邊界條件，研究了臺灣海峽，特別是其流量的變化對生態模式產生的影響。在這個生態模式中，我們假設東海的營養鹽有三個起源，即河流、台灣海峽、大陸架等。爲了估算各種不同起源的營養鹽在東海中的分佈，我們在模式中對它們進行了分別計算。它們在非線性生化項中的分離是基於它們在格子點中的濃度比。模式的計算結果表明，台灣海峽的流量變化對東海營養鹽的供給影響很大，但是對東海的初級生產的影響力不大。這是因爲從臺灣海峽流入的營養鹽的變化，可以由大陸架起源的營養鹽來補償。

(關鍵詞：臺灣海峽、東海、生態模式)

[1]日本 地球變動研究所

[2]日本 九州大學應用力學研究所